ADVANCES IN PSYCHOLOGY

119

Editors:

G. E. STELMACH

P. A. VROON

ELSEVIER
Amsterdam – Lausanne – New York – Oxford – Shannon – Tokyo

Self-Organization, Computational Maps, and Motor Control
P. Morasso and V. Sanguineti (Editors)

ARTIFICIAL FORCE-FIELD BASED METHODS IN ROBOTICS

Toshio Tsuji[1], *Pietro G. Morasso*[2], *Vittorio Sanguineti*[2]
and *Makoto Kaneko*[1]
[1]Computer Science and Systems Engineering
Hiroshima University
Kagamiyama 1-chome, Higashi-Hiroshima, 739 (JAPAN)
[2]Department of Informatics, Systems and Telecommunications
University of Genova, Via Opera Pia 13, 16145 Genova (ITALY)
e-mail : tsuji@huis.hiroshima-u.ac.jp

Abstract

In this chapter, artificial force-field based methods used in robotics are briefly reviewed with emphasis on the fact that little attention has been paid to the temporal aspects of this class of path planning methods. On the contrary, the ability to control motion time as well as the speed profile of the generated trajectories is of great interest in real-life applications. We introduce a trajectory formation technique that allows full control of the transient behavior parameters (namely, time-to-target and velocity profile).

1 Introduction

In the artificial force field approach used for the trajectory generation problem of mobile robots and robotic manipulators, such as Loeff & Soni (1975), Khatib (1986), Connolly et al. (1990), Kim & Khosla (1992), Sato (1993), Hashimoto et al. (1993), the goal is represented by an artificial attractive potential field and the obstacles by corresponding repulsive fields, so that the trajectory to the target can be

associated with the unique flow-line of the gradient field through the initial position and can be generated via a flow-line tracking process. This approach is suitable for real-time motion planning of robots since the algorithm is simple and computationally much less expensive than other methods based on global information about the task space. However, at least two important weak points should be singled out: local minima and transient control.

As regards the first problem, it is a simple observation that when the attractive potential to the goal and the repulsive one from the obstacles are equal, the gradient vector of the potential field becomes zero and the robot falls into a *deadlock*. Many methods have been proposed to overcome this problem. Connolly et al. (1990) proposed a method using the Laplace's differential equation based on the idea that the deadlock problem is completely solved when one can define a potential function which structurally does not include local minima. In fact, some potential functions of this kind have been proposed (Kim & Khosla 1992, Sato 1993, Hashimoto et al. 1993).

The other disadvantage is that in the artificial force field framework it is difficult to regulate the transient behavior of the generated trajectories such as the movement time and the shape of the velocity profile. For example, even if we use potential functions without local minima, which assure that the robot reaches the goal for any task environment, it is difficult to estimate the movement time required for reaching beforehand. Also, the velocity profile of the generated trajectory cannot be adjusted as we may require since it is determined by the shape of the potential field. Thus, contradicting the statement that a winning feature of the artificial force field approach is real-time applicability, it turns out that it is difficult to use the generated trajectory for the control of mobile robots or manipulators in real time because of this disadvantage. Quite likely, the scarce consideration about the transient behavior of the planned paths was motivated by the fact that the deadlock-free requirement was the overwhelming concern in the field.

Recently, Morasso et al. (1993, 1994) proposed a two-dimensional trajectory generation approach for modeling human reaching movements. In this method, the hand trajectory is generated by synchro-

nizing the translational and rotational velocities of the hand with a scalar signal generated by a Time Base Generator (TBG). The TBG generates a time-series, i.e. a scalar signal with a controllable finite duration and bell-shaped velocity profile. Thus, the movement time and the velocity profile of the hand trajectory can be regulated indirectly by adjusting the parameters of the TBG. Then, Tsuji et al. (1994, 1995a, 1995b) applied the TBG mechanism to the control of a non-holonomic robot and a redundant manipulator.

In this chapter, a trajectory generation technique is described by introducing the TBG into the artificial force field approach. The method can regulate the movement time from the initial position to the goal and the velocity profile of the robot. Remarkably, the method can take advantage of a variety of potential functions developed by people working in the field (particularly, the functions which are deadlock-free), because it is a property of the proposed mechanism that the temporal structure of the planned path is regulated through the TBG and is rather independent of the specific type of potential function.

2 Trajectory Generation Using Time Base Generator

2.1 Closed Loop Control System

Let us consider a trajectory generation problem with spatio-temporal constraints, which consists of moving a robot from an initial position x_0 at $t = 0$ to a target position x_d at $t = t_f$, and let us solve it by means of a closed loop control system. Figure 1 shows a block diagram of the control system, where TBG denotes the time base generator. In particular, the robot system can be described by

$$\dot{x} = g(x)u, \tag{1}$$

where $x \in \Re^l$ is the position vector of the robot and $u \in \Re^m$ is the input, and the proposed feedback controller is structured as follows:

$$u = f(e, \frac{\dot{\xi}}{\xi}), \tag{2}$$

where $e \in \Re^l$ is the error vector $e = x_d - x$ and ξ (with its time derivative $\dot{\xi}$) is the scalar signal generated by the TBG; $\xi(t)$ is defined as a first differentiable and monotonically non-increasing function satisfying $\xi(0) = 1$ and $\xi(t_f) = 0$ with t_f denoting convergence time.

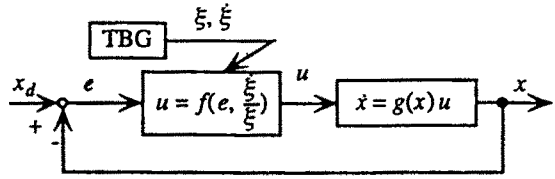

Figure 1: A block diagram of the proposed control system

2.2 Examples of TBG

In order to illustrate the operation of the TBG in the control loop, we use the *terminal attractor concept.* This special kind of attractor was introduced by Zak (1988) into a non-linear neural network model and it was shown that systems with terminal attractor dynamics always converges to the equilibrium point in a finite time, while violating the Lipschitz condition of ordinary differential equations.

Here, the following nonlinear differential equation is considered as an example of TBG with a terminal attractor:

$$\dot{\xi} = \phi(\xi) = -\gamma(\xi(1-\xi))^{\beta}, \tag{3}$$

where γ is a positive constant which allows to control the convergence time t_f, and β is a constant which determines the behavior of the TBG, with $0 < \beta < 1$. This type of TBG was originally defined for a model of human movements (Morasso et al. 1993, 1994). Morasso et al. derived the TBG with a bell-shaped velocity profile in order to represent the feature of the end-point trajectory. From (3) we can see that ξ has two equilibrium points: a stable one ($\xi = 0$) and an unstable one ($\xi = 1$). Consequently, ξ always converges stably to $\xi = 0$, when an initial value of ξ is chosen as $\xi(0) = 1 - \epsilon$, with a very small positive constant ϵ.

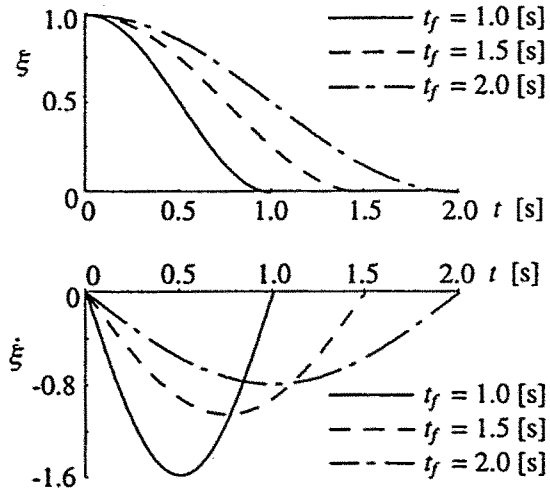

Figure 2: Change of $\xi(t)$ depending on the convergence time t_f with the constant power parameter $\beta = 0.5$

Then the convergence time t_f can be calculated as

$$t_f = \int_0^{t_f} dt \approx \int_1^0 \frac{d\xi}{\phi(\xi)} = \frac{\Gamma^2(1-\beta)}{\gamma\Gamma(2-2\beta)}, \tag{4}$$

where $\Gamma(\cdot)$ is the gamma function (Euler's integral of the second kind). Thus, the system converges to the equilibrium point $\xi = 0$ in the finite time t_f if the parameter γ is chosen as

$$\gamma = \frac{\Gamma^2(1-\beta)}{t_f\Gamma(2-2\beta)}. \tag{5}$$

Again, this means that the point is a terminal attractor.

The velocity signal $\dot{\xi}(t)$, which is null for $t = 0$ and $t = t_f$, has a bell-shaped profile with the maximum absolute value at $t = t_f/2$: $\left|\dot{\xi}(t_f/2)\right| = \gamma 4^{-\beta}$.

Figures 2 and 3 show the changes of $\xi(t)$ generated by the TBG depending on the parameters t_f and β. In Fig. 2, the time histories

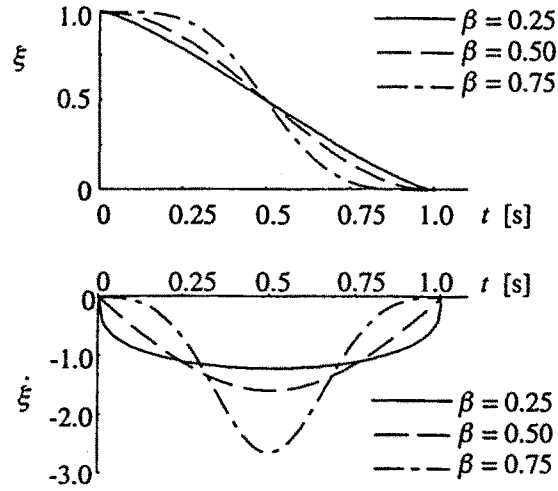

Figure 3: Change of $\xi(t)$ depending on the power parameter β with the constant convergence time $t_f = 1.0$ s

of $\xi(t)$ and $\dot{\xi}(t)$ are shown depending on the convergence time t_f = 1.0, 1.5 and 2.0 s under the parameters $\beta = 0.5$ and $\epsilon = 1.0 \times 10^{-9}$. All trajectories converge to the equilibrium point at the specified time t_f. Also, Fig. 3 shows time histories of $\xi(t)$ depending on the change of the power parameter $\beta = 0.25$, 0.5 and 0.75 with $t_f = 1.0$ s and $\epsilon = 1.0 \times 10^{-9}$. The time history of $\xi(t)$ can be regulated through the power parameter β while the convergence time remains constant.

In summary, by selecting two parameters of the TBG (t_f and β), we can generate a whole family of time-varying signals $\xi(t)$. Note that, from the point of view of real-time implementation, it is possible to use any scalar function of time satisfying the properties of $\xi(t)$ described above: half period of the cosine function, a look-up table etc.

2.3 Controller Design on the Basis of Artificial Potential Fields

In order to design the controller of Fig. 1, a differentiable potential function $V(x)$ is defined in the task space. In particular, we simply assume that at the target position x_d the potential function is zero and it is positive for any other position x. Also, we assume that the control input u is determined in such a way that the time derivative $\dot{V}$, which can be expressed as $\dot{V} = \partial V/\partial x \dot{x}$, is given by

$$\dot{V} = pV\frac{\dot{\xi}}{\xi}, \tag{6}$$

where p is a positive constant. Since $p > 0$, $V > 0$, $\xi > 0$ and $\dot{\xi} < 0$ at any t except for $t = t_f$, we have $\dot{V} < 0$, that is, asymptotic stability of the system is assured.

Equation (6) can be transformed as

$$\frac{dV}{d\xi} = p\frac{V}{\xi}. \tag{7}$$

and this differential equation can be readily solved as follows:

$$V = V_0\xi^p, \tag{8}$$

where $V_0 = V(x_0)$ is the initial value of V. Thus, we can see that the potential function is "synchronized" with the TBG because V is proportional to the pth power of ξ and since ξ reaches zero at t_f so must do V: in other words, the robot is bound to reach the target position x_d at $t = t_f$.

Figure 4 shows the time courses of V and $\dot{V}$, for a TBG described by (3). The convergence time and the power parameters of the TBG are $t_f = 1.0$ and $\beta = 0.75$, respectively, and the initial value of the potential function V_0 is $V_0 = 100$.

The first time derivative of the potential function is given by

$$\dot{V} = -\gamma p V_0 \xi^{p+\beta-1}(1-\xi)^\beta. \tag{9}$$

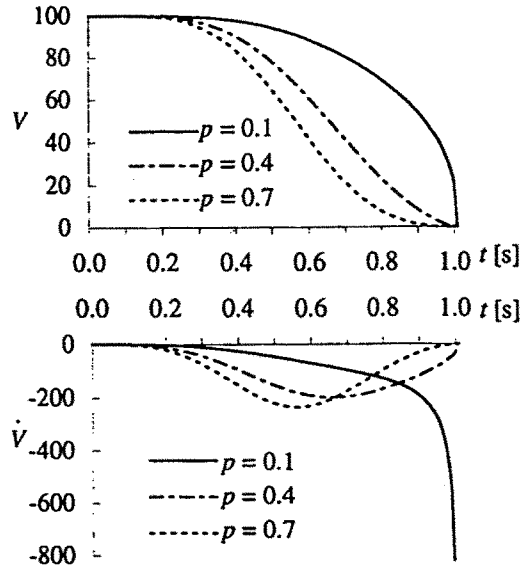

Figure 4: Change of V and $\dot{V}$ depending on the parameter p

and in the limit ($\xi \to 0$) we get $\dot{V} = -\gamma p V_0 \xi^{p+\beta-1}$, from which we can see that $\dot{V}$ converges to zero at t_f if the parameter p is selected according to $p \geq 1 - \beta$: under this condition, $\dot{V}$ is bounded along the generated trajectory.

It can be seen from Fig. 4 that V and $\dot{V}$ converge to zero at $t = 1.0$ s when $p \geq 0.25$, but $\dot{V}$ diverges at $t = 1.0$ s when $p < 0.25$; the time course of $\dot{V}$ near t_f strongly depends on p. When the parameters p and β are chosen adequately, the potential function V converges to zero at $t = t_f$ so that the robot can reach the target position at the desired time.

3 Trajectory Generation of a Unicycle-like Vehicle

In this section, we show how the general approach described in the previous section can be applied to robot control problems with complex kinematic constraints, as in the navigation of non-holonomic vehicles. In fact, control of mobile robots with nonholonomic constraints has received a great deal of attentions (Li & Canny 1993). For the closed loop control on the basis of a kinematic model of a mobile robot, Samson (1991) and Pomet (1992) proposed a feedback law using periodic time functions and showed that the mobile robot with two driving wheels can be positioned to the given final configuration for any initial condition. Although the smooth time-varying feedback of this approach can assure the stability of the system, slow convergence is a practical defect. Then, Canudas de Wit & Sørdalen (1992) proposed a piecewise smooth feedback law,using a discontinuous controller and proved the exponential stabilization of the mobile robot as well as the extreme improvement of the convergence speed to the target point, with respect to time-varying smooth feedback control. Also, Badreddin & Mansour (1993) showed that a special choice of the polar coordinate system representing the position and orientation of the mobile robot allows to derive a smooth stabilizing control law without contradicting the well known work of Brockett (1983). Casalino et al. (1994) derived the effective closed loop control law in the framework of the Lyapunov stability theory, which can assure the global stability. In this section, the trajectory generation method using the TBG is applied to a unicycle-like vehicle, that is a mobile robot with two driving wheels.

3.1 Model of a Unicycle-like Vehicle

Figure 5 shows a unicycle-like vehicle, where Σ_w denotes the world coordinate system (for a planar task space) and Σ_c the moving coordinate system fixed to the vehicle (with the origin of Σ_c set symmetrically among the wheels and the x_c axis oriented as the direction of motion of the vehicle). Thus, we can choose the following generalized coordi-

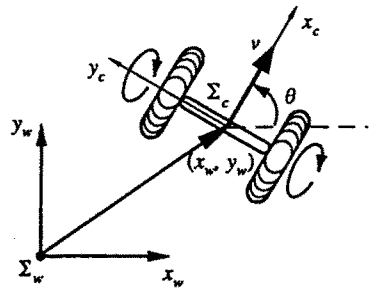

Figure 5: A unicycle-like vehicle

nates of the vehicle: position (x_w, y_w) and orientation angle θ of Σ_c with respect to Σ_w.

The kinematics of the vehicle can be described by the following relationship between the time derivative of the generalized coordinate vector $x = (x_w, y_w, \theta)^T$ and the linear and the angular velocities of the vehicle $u = (v, \omega)^T$:

$$\dot{x} = G(x)u, \tag{10}$$

where

$$G(x) = \begin{bmatrix} \cos\theta & 0 \\ \sin\theta & 0 \\ 0 & 1 \end{bmatrix} \tag{11}$$

and the following kinematic constraint must be satisfied (it can be easily derived from equation 10):

$$\dot{x}_w \sin\theta - \dot{y}_w \cos\theta = 0. \tag{12}$$

3.2 Derivation of the Control Law

Our purpose is to derive a control law that automatically drives the vehicle from the initial configuration to the target configuration. Without any loss of generality, the origin of the world coordinate system Σ_w can be set at the target position, with the x_w axis directed as the desired final orientation of the vehicle (Fig. 6).

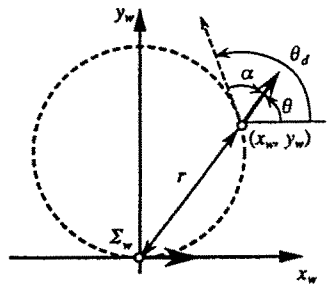

Figure 6: Coordinate transformation

The piecewise smooth feedback control law proposed by Canudas de Wit & Sørdalen (1992) uses the family of circles that pass through the origin and the current position of the vehicle and contacts with the x_w axis at the origin as shown in Fig. 6. In the figure, θ_d represents the tangential direction of this circle at the position x and it belongs to $[-\pi, \pi)$. Their control law is based on the idea that the arc length from the origin to the current position should be decreasing and the current angular orientation of the vehicle should agree with the tangential direction θ_d. In our approach the distance r from the current position to the origin is used, instead of the arc length.

Let α denote the angle between the tangential direction θ_d and the current angular orientation θ, with the intention of designing a control law which can eliminate this kind of *orientation error* together with the corresponding *positional error* denoted by the distance r from the target. The following coordinate transformation from $x = (x_w, y_w, \theta)^T$ to $z = (r, \alpha)^T$ is then introduced (Canudas de Wit & Sørdalen 1992):

$$r(x_w, y_w) = \sqrt{{x_w}^2 + {y_w}^2} \tag{13}$$

$$\alpha(x_w, y_w, \theta) = e + 2n(e)\pi \tag{14}$$

where

$$e = \theta - \theta_d, \tag{15}$$

$$\theta_d = 2\text{atan2}(y_w, x_w), \tag{16}$$

and $n(e)$ is a function that takes an integer in order to satisfy $\alpha \in [-\pi, \pi)$. Also, atan2$(\cdot,\cdot)$ is a scalar function defined as atan2$(a,b) = \arg(b + ja)$, with j denoting the imaginary unit and arg the argument of a complex number. As a result of such coordinate transformation $z = F(x)$, the target configuration of the vehicle can be expressed as $z_f = (0,0)^T$.

Thus, in order to derive the control law which can stabilize the system to the target, we can write, first, the relationship between $\dot{z}$ and $\dot{x}$

$$\dot{z} = \frac{\partial F(x)}{\partial x}\dot{x} = J(x)\dot{x}, \tag{17}$$

where

$$J(x) = \begin{bmatrix} x_w(x_w{}^2 + y_w{}^2)^{-1/2} & y_w(x_w{}^2 + y_w{}^2)^{-1/2} & 0 \\ 2y_w(x_w{}^2 + y_w{}^2)^{-1} & -2x_w(x_w{}^2 + y_w{}^2)^{-1} & 1 \end{bmatrix} \in \Re^{2\times 3}. \tag{18}$$

Substituting (10) into (17), we have the relationship between $\dot{z}$ and the system input u:

$$\dot{z} = J(x)G(x)u = B(x)u, \tag{19}$$

where

$$B(x) = \begin{bmatrix} b_1 & 0 \\ b_2 & 1 \end{bmatrix}, \tag{20}$$

$$b_1(x) = (x_w{}^2 + y_w{}^2)^{-1/2}\,(x_w \cos\theta + y_w \sin\theta), \tag{21}$$

$$b_2(x) = 2(x_w{}^2 + y_w{}^2)^{-1}(y_w \cos\theta - x_w \sin\theta). \tag{22}$$

Thus, the number of state variables is reduced to the same number as the system input and for this system the following potential function can be defined:

$$V = \frac{1}{2}\left(k_r r^2 + k_\alpha \alpha^2\right), \tag{23}$$

where k_r and k_α are positive constants. By differentiating the above equation and taking into account (19), we obtain

$$\dot{V} = k_r r\dot{r} + k_\alpha \alpha\dot{\alpha} = k_r b_1 r v + k_\alpha \alpha\,(b_2 v + \omega)\,. \tag{24}$$

On the other hand, for the potential function (23), equation (6) reduces to

$$\dot{V} = \frac{p}{2}\left(k_r r^2 + k_\alpha \alpha^2\right)\frac{\dot{\xi}}{\xi}. \tag{25}$$

Comparing (24) with (25), we can derive the following control law for coordinated speed and steering :

$$u = \begin{bmatrix} v \\ \omega \end{bmatrix} = \begin{bmatrix} \frac{pr(x)\dot{\xi}(t)}{2b_1(x)\xi(t)} \\ -b_2(x)v + \frac{p\alpha(x)\dot{\xi}(t)}{2\xi(t)} \end{bmatrix}, \tag{26}$$

where it is assumed that $b_1 \neq 0$ for any t except for $t = t_f$.

Substituting the control law (26) into the system equation (19), we have

$$\dot{r} = b_1 v = \frac{pr\dot{\xi}}{2\xi}, \tag{27}$$

$$\dot{\alpha} = b_2 v + \omega = \frac{p\alpha\dot{\xi}}{2\xi}, \tag{28}$$

from which we obtain

$$\frac{dr}{d\xi} = \frac{pr}{2\xi}, \tag{29}$$

$$\frac{d\alpha}{d\xi} = \frac{p\alpha}{2\xi}. \tag{30}$$

Solving this differential equation, we can get

$$r = r_0 \xi^{\frac{p}{2}}, \tag{31}$$

$$\alpha = \alpha_0 \xi^{\frac{p}{2}}, \tag{32}$$

where r_0 and α_0 are the initial values of r and α, respectively. Thus it can be seen that the *distance error* r and the *angular error* α decrease as the $(\frac{p}{2})$th power of ξ under the control law (26).

In summary, the system equation (19) reduces to

$$\dot{r} = \frac{pr_0}{2}\xi^{\frac{p}{2}-1}\dot{\xi}, \tag{33}$$

$$\dot{\alpha} = \frac{p\alpha_0}{2}\xi^{\frac{p}{2}-1}\dot{\xi} \tag{34}$$

and if the control variable ξ goes down to 0 according to (3), we can see that $p \geq 2(1-\beta)$ is required for keeping bounded the values of $\dot{r}$ and $\dot{\alpha}$.

3.3 Computer Simulations

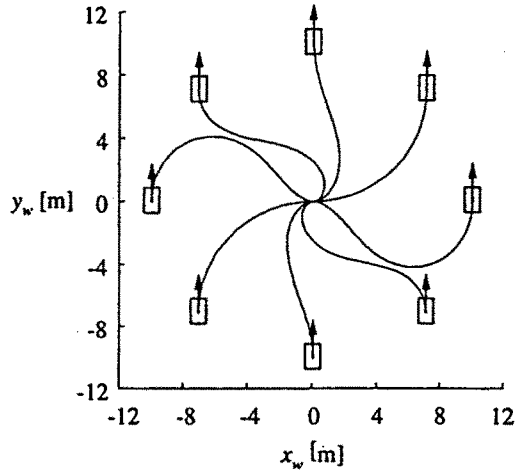

Figure 7: Trajectories generated by the control law when the vehicle is initially located on a circle in the x_w–y_w plane with $\theta_0 = \pi/2$ rad. (The arrow denotes the initial orientation θ_0.)

3.3.1 Generation of Curved Trajectories Figures 7 and 8 show the results generated by the proposed method of coordinated speed-steering control, for several initial conditions located at different points on a circle, with a 10 m radius: the initial orientation angle θ_0 is $\pi/2$ in Fig. 7 and 0 in Fig. 8, respectively. The TBG parameters are: $t_f = 1.0$ s, $p = 2$, $\beta = 0.75$.

It can be observed that the control law (26) becomes singular when the term $b_1(x)$ goes to 0 and from (21) it is clear that such singularity occurs in the case that the orientation vector of the vehicle is orthogonal with respect to the vector which joins the current to the target position. We tested the robustness of the control mechanism in the neighborhood of the singular configurations, by carrying out a number of simulations with initial conditions very close to singularity. Some of them are included in Fig. 7 and 8: two trajectories starting from locations close

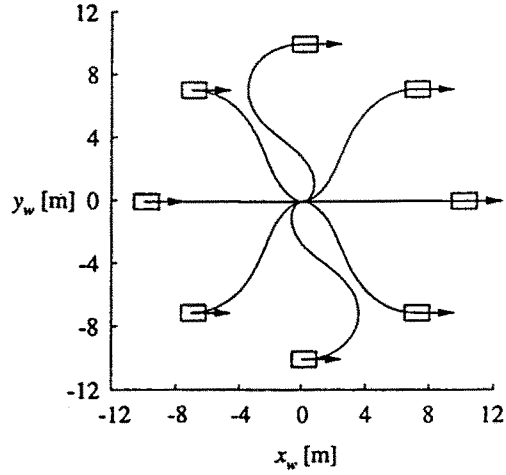

Figure 8: Trajectories generated by the control law when the vehicle is initially located on a circle in the x_w-y_w plane with $\theta_0 = 0$ rad. (The arrow denotes the initial orientation θ_0.)

to the x_w axis in Fig. 7 ($x_0 = [10\text{m}, 1.0 \times 10^{-5}\text{m}, \pi/2\text{rad}]^T$ and $x_0 = [-10\text{m}, -1.0 \times 10^{-5}\text{m}, \pi/2\text{rad}]^T$), and two trajectories starting from points close to the y_w axis in Fig. 8 ($x_0 = [1.0 \times 10^{-5}\text{m}, 10\text{m}, 0\text{rad}]^T$ and $x_0 = [-1.0 \times 10^{-5}\text{m}, -10\text{m}, 0\text{rad}]^T$). In all cases we observed that the actual trajectories are repulsed from the singular configuration and the vehicle can arrive at the target position in a smooth way, without any forward/backward oscillatory movement.

We can also observe that the trajectories from the initial configurations $x_0 = [5\sqrt{2}\text{m}, 5\sqrt{2}\text{m}, \pi/2\text{rad}]^T$ and $x_0 = [-5\sqrt{2}\text{m}, -5\sqrt{2}\text{m}, \pi/2\text{rad}]^T$ of Fig. 7 appear to be circular. In fact, it is possible to prove their circularity in a formal way. Let us suppose that the initial orientation θ_0 agrees with the tangential direction of the circle passing through the initial position and the origin, as in Fig. 9. From (14) we have $\alpha_0 = 0$ and thus, taking into account (26), we obtain

$$\omega = -b_2(x)v. \tag{35}$$

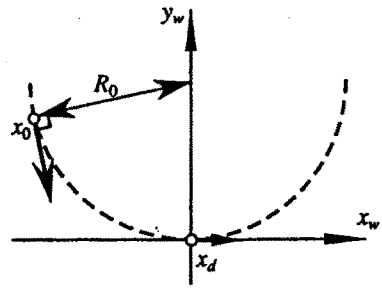

Figure 9: Generation of a circular trajectory

If we denote with R_0 the radius of the circle defined at the initial position, we have

$$R_0 = \frac{{x_{w0}}^2 + {y_{w0}}^2}{2y_{w0}}, \tag{36}$$

and using simple trigonometric relations ($\sin\theta = x_w/R_0$ and $\cos\theta = (R_0 - y_w)/R_0$) we can transform the (22) expression of the $b_2(x)$ gain in the following way

$$b_2 = \frac{2}{{x_w}^2 + {y_w}^2}\left(\frac{R_0 - y_w}{R_0}y_w - \frac{x_w}{R_0}x_w\right) = -\frac{1}{R_0}, \tag{37}$$

which tells us that in this situation such gain becomes a constant. As a consequence, the vehicle approaches the target sliding on the circle and reaches it in the planned convergence time. For such special case of circular paths, Fig. 10 shows the time histories of the x_w coordinate and the linear velocity v (initial configuration $x_0 = [5\sqrt{2}\text{m}, 5\sqrt{2}\text{m}, \pi/2\text{rad}]^T$, as in Fig. 7). In particular, the output of the proposed controller (solid line) is compared with the results of the method by Canudas de Wit & Sørdalen (1992) (dashed line) and we can see that while the latter method tends to approach the target with a progressive slowing down after an initial jerk, our method generates a smoother time series with an approximately bell-shaped profile which converges to the target in the appointed time t_f.

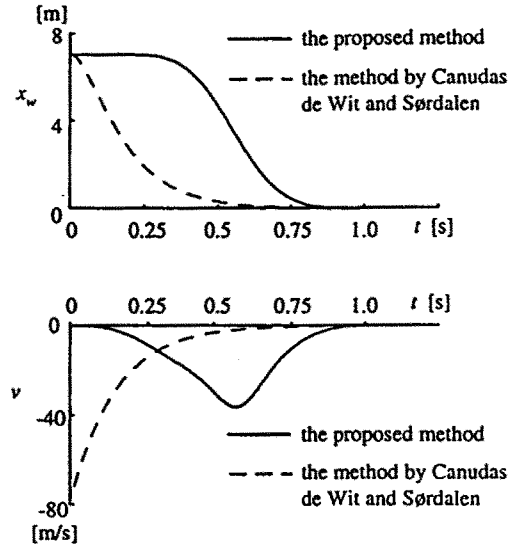

Figure 10: Time histories of x_w and v where the initial position of the vehicle is $x_0 = [5\sqrt{2}\text{m}, 5\sqrt{2}\text{m}, \pi/2\text{rad}]^T$

3.3.2 Response to External Disturbances At first sight, the proposed method might appear to be a kind of the open loop control if we consider that, as the consequence of the control law, the resulting path is described by (31) and (32). However, this is not the case, as it is clearly shown by the simulation illustrated in Fig. 11, in which an external disturbance was applied during movement, suddenly displacing the position of the vehicle. After the vehicle starts from the same initial configuration of Fig. 10, the x_w coordinate is externally changed to $x_w = 8$ m at time $t = 0.5$ s and it can be seen that the resulting trajectory, following the disturbance but keeping the same control law, is still able to smoothly converge to the target in the planned time.

In fact, the initial values r_0 and α_0 which appear in (31) and (32) are not computed explicitly in our method but are natural consequences of the feedback control law, which is able to compensate the effect of the external disturbance. Accordingly, even if equations (31) and (32)

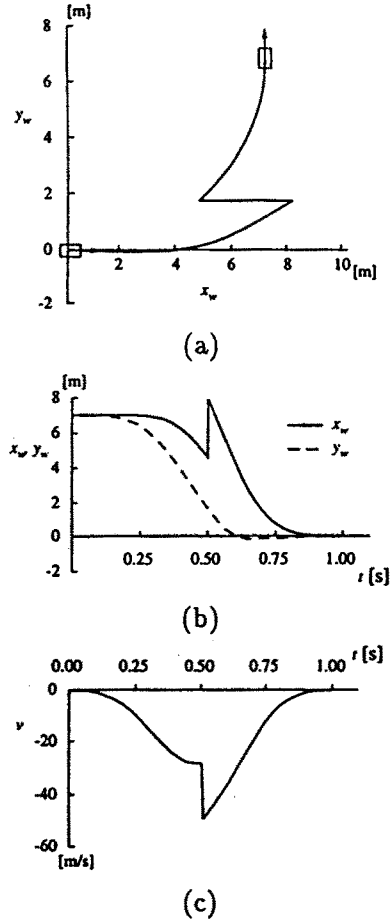

Figure 11: Generated trajectory when the position of the vehicle is disturbed externally at $t = 0.5$ s

are violated by applying the external disturbance, the proportional relationship itself is preserved and the vehicle converges to the target position at the time t_f specified in the TBG.

4 Conclusions

In this chapter we discussed an approach which allows force field based mechanisms of trajectory formation to have a controllable temporal transient. As an example, we applied it to the control of non-holonomic unicycle-like vehicles but its range of application is quite large. In particular, it can play an important role in the coordination of multiple robots where trajectory interference is intrinsically a spatio-temporal phenomenon.

The relevance in biological motor control is multi-faceted. In previous chapters the dynamics of cortical maps is considered from the point of view of field computation. Thus, all the dynamic phenomena which may be interpreted as processes of flow-line tracking, in a field with point or region attractors, may well be guided and time-controlled via the TBG mechanism: it is sufficient to modulate the relaxation gain with the TBG variables. An important side-effect is that it allows the synchronization of a number of loosely coupled dynamic processes which are occurring in different cortical maps, whatever the shape and the metric of the respective fields. On a higher hierarchical level, the same mechanism might operate in problems of bimanual coordination, which require accurate timing of two quasi-independent motor control sub-system.

As regards the biological implementation of the TBG, if we consider that it is also responsible for starting the trajectory formation process, we can speculate that a plausible site is in the subcortical structures, particularly in the circuits which receive information from different cortical areas (striatum $\rightarrow$ pallidus $\rightarrow$ thalamus) and then loop back to the cortex. This loop, which has a mainly excitatory nature, is modulated by the inhibitory influence coming from another nucleus (substantia nigra) via dopaminergic synapses. Deficiencies of this neurotransmitter

are known to be involved in the motor impairments of the Parkinson syndrome, which include slowness and difficulty to initiate movements. Symptoms which are compatible with a malfunctioning TBG.

Acknowledgment

The authors would like to express their sincere thanks to T. Yamanaka for the development of computer programs.

References

Badreddin, E. & Mansour, R. (1993). Fuzzy-tuned state feedback control of a nonholonomic mobile robot, *IFAC World Congress*, Vol. 6, pp. 577–580.

Brockett, R. W. (1983). Asymptotic stability and feedback stabilization, *in* Brockett, Millmann & Sussmann (eds), *Differential Geometric Control Theory*, Birkhauser, pp. 181–191.

Canudas de Wit, C. & Sørdalen, O. J. (1992). Exponential stabilization of mobile robots with nonholonomic constraints, **37**: 1791–1797.

Casalino, G., Aicardi, M., Bicchi, A. & Balestrino, A. (1994). Closed-loop steering for unicycle-like vehicles: A simple lyapunov like approach, *Preprint of the Fourth IFAC Symposium on Robot Control*, pp. 335–342.

Connolly, C. I., Burns, J. B. & Weiss, R. (1990). Path planning using laplace's equation, *Proceedings of the IEEE International Conference on Robotics and Automation*, pp. 2102–2106.

Hashimoto, H., Kunii, Y., Harashima, F., Utkin, V. I. & Drakunov, S. V. (1993). Obstacle avoidance control of multi-degree-of-freedom manipulator using electrostatic potential field and sliding mode, *Journal of the Robotics Society of Japan* **11**(8): 1220–1228.

Khatib, O. (1986). Real-time obstacle avoidance for manipulators and mobile robots, *International Journal of Robotics Research* 5(1): 90–98.

Kim, J. O. & Khosla, K. (1992). Real-time obstacle avoidance using harmonic potential functions, *IEEE Transactions on Robotics and Automation* 8(3): 338–349.

Li, Z. & Canny, J. F. (eds) (1993). *Nonholonomic motion planning*, Kluwer Academic Pub.

Loeff, L. A. & Soni, A. H. (1975). An algorithm for computer guidance of a manipulator in between obstacles, *Transsactions of ASME, Journal of Engineering for Industry* 97(3): 836–842.

Morasso, P. G., Sanguineti, V. & Tsuji, T. (1993). A dynamical model for the generator of curved trajectories, *Proceedings of the International Conference on Artificial Neural Networks*, pp. 115–118.

Morasso, P. G., Sanguineti, V. & Tsuji, T. (1994). A model for the generation of virtual targets in trajectory formation, *in* Faure, Keuss, Lorette & Vinter (eds) , *Advances in handwriting and drawing: a multidisciplinary approach*, Europia, Paris, pp. 333-348.

Pomet, J. B. (1992). Explicit design of time varying stabilizing feedback laws for a class of controllable systems without drift, *System and Control Letters* 18: 139–145.

Samson, C. (1991). Velocity and torque feedback control of a nonholonomic cart, *Advanced Robot Control, Lecture Notes in Control and Information Sciences* 162: 125–151.

Sato, K. (1993). Global motion planning using a laplacian potential field, *Journal of the Robotics Society of Japan* 11(5): 702–709.

Tsuji, T., Morasso, P. & Kaneko, M. (1995a). Feedback control of nonholonomic mobile robots using time base generator, *Proceedings of IEEE International Conference on Robotics and Automation 1995*, pp. 1385–1390.

Tsuji, T., Morasso, P., Shigehashi, K. & Kaneko, M. (1995b). Motion planning for manipulators using artificial potential field approach that can adjust convergence time of generated arm trajectory, *Journal of the Robotics Society of Japan* **13**(3): 125–130. In Japanese.

Tsuji, T., Morasso, P., Yamanaka, T. & Kaneko, M. (1994). Feedback control of mobile robots with nonholonomic constraints using time base generator, *Journal of the Robotics Society of Japan* **12**(7): 1072–1078. In Japanese.

Zak, M. (1988). Terminal attractors for addressable memory in neural networks, *Physics Letters A* **133**: 218–222.